

Electrochemical Biosensor Based on Myoglobin for Trichloroacetic Acid and Nitrite Determination

Guiling Luo¹, Hui Xie¹, Hamza Abdalla Yones¹, Si Mi¹, Binghang Li¹, Yubao Wang¹, Pengying Chen¹, Guangjiu Li², Wei Sun^{1*}

¹ Key Laboratory of Water Pollution Treatment & Resource Reuse of Hainan Province, Key Laboratory of Functional Materials and Photoelectrochemistry of Haikou, College of Chemistry and Chemical Engineering, Hainan Normal University, Haikou 571158, P R China

² Key Laboratory of Optic-electric Sensing and Analytical Chemistry for Life Science of Ministry of Education, College of Chemistry and Molecular Engineering, Qingdao University of Science and Technology, Qingdao 266042, China

*E-mail: sunwei@hainnu.edu.cn

Received: 6 April 2019 / *Accepted:* 27 June 2019 / *Published:* 31 July 2019

In this paper the effect of gold nanochains (AuNCs) on direct electron transfer of Myoglobin (Myb) was studied in detail. A Nafion polymer dispersions, Myb solution and AuNCs solution were dropped on carbon ionic liquid electrode (CILE) in sequence to develop a new working electrode. AuNCs have high electrochemical activity with excellent biocompatibility, which serve as electron transfer path for intensifying electrochemical response of Myb. In electrolyte a pair of symmetrical redox peaks of Myb was displayed on cyclic voltammogram and electrochemical performance of this modified electrode was investigated. Myb on electrode surface exhibited good electrocatalytic reduction activity to trichloroacetic acid (TCA) and sodium nitrite (NaNO₂). The electrocatalytic current displayed a linearity regression behavior to TCA concentrations from 2.0 to 400.0 mmol/L with the detection limit of 0.26 mmol/L, to NaNO₂ concentrations from 0.04 to 1.8 mmol/L with the detection limit of 0.013 mmol/L. Consequently, this paper extended the utilization of AuNCs in construction of an excellent platform based on electrocatalysis of redox enzymes.

Keywords: Gold nanochains; Direct electrochemistry; Myohemoglobin; Electrocatalysis

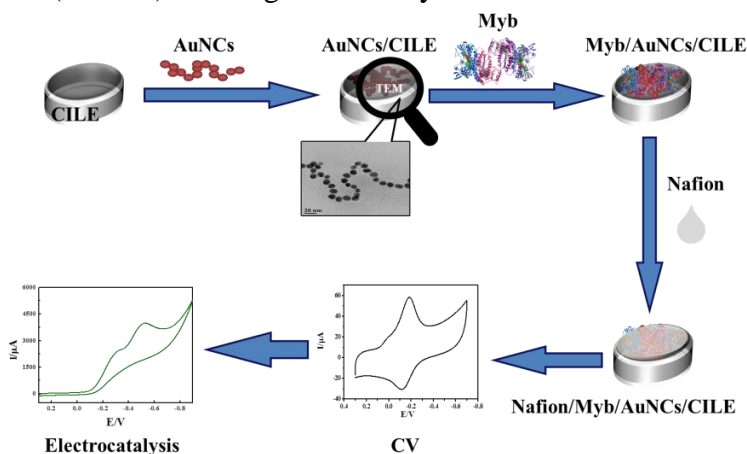
1. INTRODUCTION

Myohemoglobin (Myb) is a crucial oxygen conveying protein in the organism, which is made up of pro-alpha polypeptide chain and heme co-factor [1, 2]. Whereas, because electroactive center in the sophisticated structure of Myb and inactivation of Myb on bare electrode, direct electron transfer (DET) of Myb on non-modified electrode is hard to be implemented [3]. Significant trials have been fabricated to enhance DET rates of proteins with modified electrodes by employed intermediaries,

such as didodecyldimethylammonium bromide [4], hexagonal boron nitride nanosheet [5], graphene and dsDNA composite [6], ionic liquid-graphene-cobalt oxide nanoflower composite [7]. By employing these mediators, DET of redox proteins can be highly improved on the working electrodes with good-shaped redox peaks displayed in cyclic voltammograms.

Gold nanoparticles (AuNPs) have served as conductive centers to promote the DET process of redox enzyme [8]. Self-assembling of AuNPs into different formations has got great attentions due to their corporation capabilities that arise from electronic properties [9]. Notably, various microstructures of AuNPs, such as nanowires [10], nanorods [11], nanochains [12] and nanocages [13] engage more interests owing to stability, renewability and biocompatibility [14, 15]. AuNPs with one-dimensional chain structure have exhibited many advantages than single particles or aggregates. However, seldom reports have been associated with the implement of gold nanochains (AuNCs) in the field of biosensors. Sinha et al. demonstrated the catalytic activity of AuNCs for the reduction of nitrobenzol to aniline and methylene blue to leuco methylene blue, which was ascribed to the well-organized chains structure that regulated the electron transfer [16].

In this work, AuNCs were used for the improvement of DET rates of Myb by modification on carbon ionic liquid electrode (CILE). Myb and AuNCs decorated electrode was constructed and Nafion was applied to fix the composite on CILE. More importantly, the unique chain structure of AuNCs can enhance the immobilized amount of Myb with fast electron transfer path, which may improve the sensitivity of electroanalysis. The procedure for construction of Nafion/Myb/AuNCs/CILE was illustrated in Scheme 1 and DET of Myb on AuNCs based working electrode was realized by cyclic voltammetry (CV) with good-shaped and symmetrical peaks. This Myb based electrochemical biosensor illustrated well electro-reduction ability to trichloroacetic acid (TCA) and sodium nitrite (NaNO_2) with high sensitivity.



Scheme 1. Construction of Nafion/Myb/AuNCs/CILE and electrocatalysis.

2. EXPERIMENTAL

2.1 Reagents

Myb (Sigma, USA), 1-hexylpyridinium hexafluorophosphate (HPPF₆, Lanzhou Yulu Fine Chem. Co., China), Nafion (minimum 5% polymer dispersions, Beijing Honghaitian Technology Ltd.

Co., China), AuNCs (2.33 nmol/L solution, average particle size 15 nm, Nanjing XFNANO Mater. Co., China), graphite powder ($\leq 30 \mu\text{m}$, Shanghai Colloid Chem. Plant, China), TCA (Shanghai Aladdin Industrial Co., China) and NaNO_2 (Shanghai Chem. Plant, China) were employed as got. 0.1 mol/L phosphate buffer solutions (PBS) with varieties of pH were prepared with ultrapure water and deoxygenated for 30 min before use.

2.2 Apparatus

CHI 604E electrochemical workstation (Shanghai CH Instrument, China) was employed for electrochemical experiments, which was equipped with Nafion/Myb/AuNCs/CILE ($\Phi=4.0 \text{ mm}$) as working electrode, platinum wire as counter electrode and saturated calomel electrode (SCE) as reference electrode. Scanning electron microscopy (SEM) was recorded with JSM-7100F (Japan Electron, Japan) with transmission electron microscopy (TEM) on JEM-2100F (Japan Electron, Japan). Fourier transform infrared (FT-IR) spectrum and ultraviolet-visible (UV-Vis) absorption spectrum were achieved on Nicolet 6700 FT-IR spectrometer (Thermo Fisher, USA) and TU-1901 double-beam UV-Visible spectrophotometer (Purkinje, China).

2.3 Preparation of Nafion/Myb/AuNCs/CILE

CILE was home-made on the basis of commonly used routine [17] with HPPF_6 and graphite power, which was burnished smoothly before use. Then $6.0 \mu\text{L}$ of 2.33 nmol/L AuNCs solution was dropped on CILE and air-dried. After that Myb were modified on the electrode surface by dropping $8.0 \mu\text{L}$ of 15.0 mg/mL Myb solution on AuNCs/CILE. Lastly, $6.0 \mu\text{L}$ of 0.5% Nafion solution was casted on Myb/AuNCs/CILE, which could form a stable membrane and immobilize Myb on the electrode. The modified electrode was called as Nafion/Myb/AuNCs/CILE. Other working electrodes such as Nafion/Myb/CILE, Nafion/AuNCs/CILE etc. were fabricated by the same process.

2.4 Electrochemical measurement

CV experiments of various working electrodes were investigated in a 0.1 mol/L PBS. Three electrode system was put in electrolytic cell containing 0.1 mol/L pH 2.0 PBS with controlled potential swept from 0.3 to -0.7 V (vs. SCE) at the scan rate of 100 mV/s for DET investigation. Electrochemical impedance spectroscopic (EIS) experiments were performed in a 10.0 mmol/L $[\text{Fe}(\text{CN})_6]^{3-/4-}$ and 0.1 mol/L KCl solution.

3. RESULT AND DISCUSSION

3.1 Characteristics of AuNCs

AuNCs used were checked by SEM with the image shown in Fig. 1A, which displayed a representative regular chains model with a longer one-dimensional configuration. Therefore the active

surface of the modified electrode was increased greatly. The morphology of AuNCs was further illustrated by TEM (Fig. 1B), which proved that AuNCs were composed of uniform gold nanoparticles (average diameter of 15 nm) that evenly distributed and connected to get a chain-shape. Therefore the electron can be transferred along the chain structure of conductive metal AuNPs to form a long distance communication.

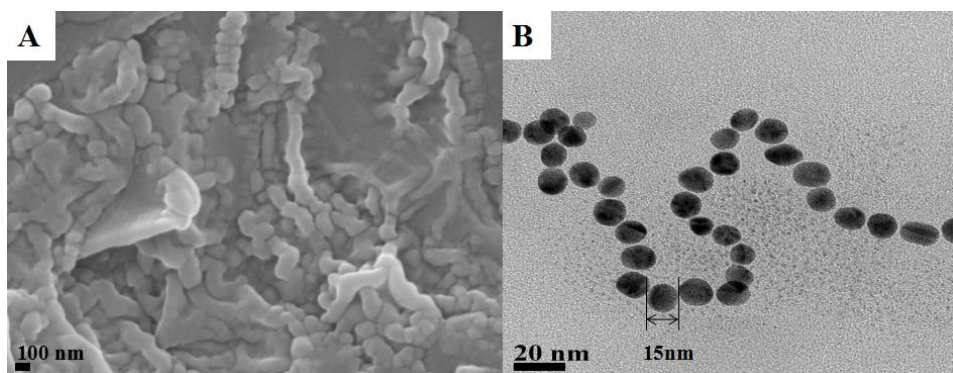


Figure 1. SEM (A) and TEM (B) images of AuNCs

3.2 Spectroscopic results

FT-IR characteristic peaks of Myb has been reported with the intension and width of the characteristic absorption bands minified or vanished away after denaturation [18,19]. The amide I and II absorption peaks of Myb mixed with AuNCs appeared at 1645 and 1526 cm^{-1} (Fig. 2A b), which had similar positions with inherent peaks of Myb at 1649 and 1529 cm^{-1} (Fig. 2A a). The result displayed that the inherent constitution of Myb was not varied after mixed with AuNCs. UV-Vis absorption spectrum of Myb was reported with Soret band occurred at 408.5 nm (curve a). While the mixture of Myb with AuNCs illustrated the similar absorption peaks as that of Myb, which noted that Myb in the mixture reserved its inherent framework due to the biocompatibility of AuNCs [20].

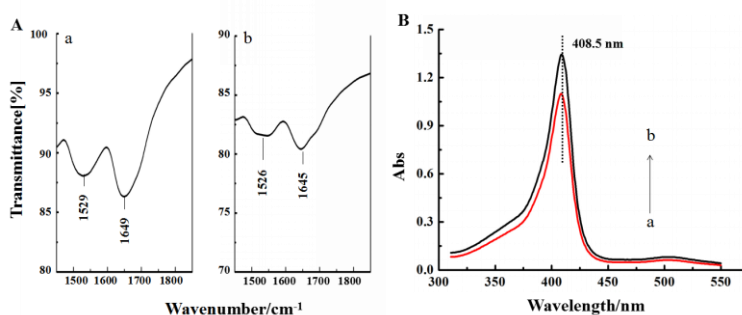


Figure 2. (A) FT-IR spectra of (a) Myb; (b) AuNCs-Myb composite; (B) UV-Vis spectra of native Myb (curve a) and AuNCs-Myb mixture (curve b) solution with water.

3.3 EIS of the modified electrodes

EIS of various working electrodes were shown in Fig. 3. The electron-transfer resistance (R_{et}) data of Nafion/CILE (curve c) and Nafion/AuNCs/CILE (curve b) was got as 45.43 Ω and 10.36 Ω , indicating that AuNCs accelerated the electron transfer on modified electrode. When Nafion and Myb were dropped on CILE, the R_{et} value was observed as 61.67 Ω (curve c). The reason was owing to the presence of Myb impeded the diffusion of $[\text{Fe}(\text{CN})_6]^{3-/4-}$ toward the electrode interface. When AuNCs was dropped on the electrode, the R_{et} data was markedly decreased to 36.53 Ω (curve a). AuNCs has metal conductivity with the ability of long distance transfer, which can serve as an electron-transfer intermediary between electrolyte and the working electrode. Therefore the electron transfer rate of $[\text{Fe}(\text{CN})_6]^{3-/4-}$ on the AuNCs/CILE was improved.

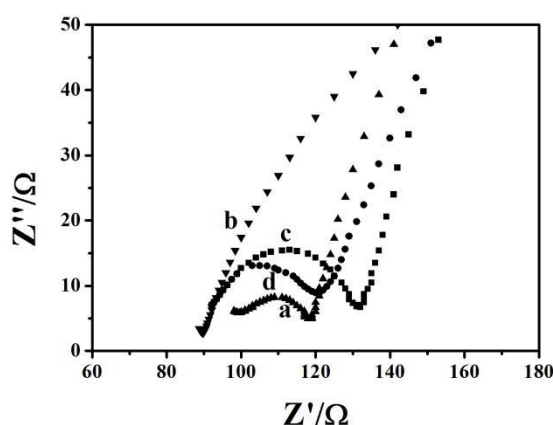


Figure 3. EIS of (a) Nafion/Myb/AuNCs/CILE, (b) Nafion/AuNCs/CILE, (c) Nafion/CILE, and (d) Nafion/Myb/CILE in 10.0 mmol/L $[\text{Fe}(\text{CN})_6]^{3-/4-}$ and 0.1 mol/L KCl solution.

3.4 Voltammetric characteristic of Nafion/Myb/AuNCs/CILE

Voltammetric response of the immobilized Myb was carefully checked by CV in a deaerated pH 2.0 PBS (Fig. 4A). On Nafion/CILE (curve a) and Nafion/AuNCs/CILE (curve b) stable electrochemical background displayed, which illustrated that almost no electro-active molecules present on the electrode. On Nafion/Myb/CILE (curve c) an asymmetric redox peaks was observed on CV with the reduction peak current (I_{pc}) as 42.23 μA and the oxidation peak current (I_{pa}) as 27.57 μA . The results revealed that DET between Myb and CILE was got with low DET rate, which was in agreement with reference [21]. After casted AuNCs on the electrode, the current enhanced obviously than that of Nafion/Myb/CILE with a pair of symmetric peak appeared (curve d). The redox currents were obtained as 76.33 μA (I_{pc}) and 83.09 μA (I_{pa}), which was approximately 2.4 times higher than Nafion/Myb/CILE. From curve d the value of oxidation potential (E_{pa}) and reduction potential (E_{pc}) were got as -0.237 V and -0.151 V. The formal peak potential ($E^{0'}$) was calculated as -0.194 V (vs. SCE). So the presence of high conductive and chain-like AuNCs played an essential role in building a

fast electron transfer path to improve the DET of Myb with the modified electrode. Therefore, DET of Myb was successfully achieved and accelerated on AuNCs modified CILE.

The effect of scan rate (v) on the voltammetric behavior of Nafion/Myb/AuNCs/CILE was researched by CV (Fig. 4B). A pair of well-proportioned redox peaks achieved in the scan rate from 100 to 1000 mV/s with the currents increasing. The relationships were established with two linear formula as $I_{pc}(\mu A) = 536.7v(V/s) + 40.22$ ($n=20$, $\gamma=0.996$) and $I_{pa}(\mu A) = -464.8v(V/s) - 26.53$ ($n=20$, $\gamma=0.996$). Therefore the voltammetric response of Nafion/Myb/AuNCs/CILE was an absorption-controlled process, in which the Myb·Fe(III) were reduced to Myb·Fe(II) and then fully reoxidized to Myb Fe(III). Two lines were derived with the equations as $E_{pa}(V) = 0.036 \ln v(V/s) - 0.064$ ($n=8$, $\gamma=0.993$) and $E_{pc}(V) = -0.041 \ln v(V/s) - 0.29$ ($n=8$, $\gamma=0.98$). The related parameters can be counted based on Laviron's equations [22] with the data of electron transfer coefficient (α), electron transfer rate constant (k_s) and n as 0.47, 0.76 s^{-1} and 1.16. This k_s value was large than that of Myb on CTS/Myb-IL-GR-Co₃O₄/CILE (0.675 s^{-1}) [7], BP-PEDOT:PSS/CILE (0.56 s^{-1}) [23] and Nafion-Myb-BMIMPF₆/CPE (0.36 s^{-1}) [24]. So the DET of Myb was fasted because of specific interface supplied by AuNCs on working electrode.

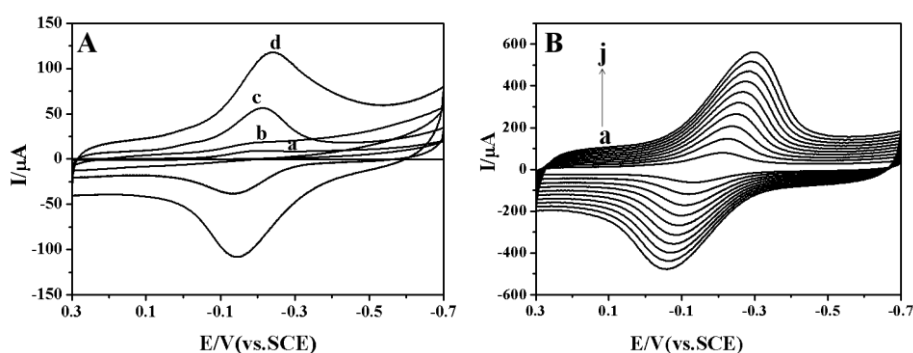


Figure 4. (A) CVs of (a) Nafion/CILE, (b) Nafion/AuNCs/CILE, (c) Nafion/Myb/CILE and (d) Nafion/Myb/AuNCs/CILE in pH 2.0 PBS at 100 mV/s; (B) CVs of Nafion/Myb/AuNCs/CILE in pH 2.0 PBS with different v . (from a to j: 100, 200, 300, 400, 500, 600, 700, 800, 900, 1000 mV/s)

The surface concentration (Γ^*) of electrochemical active Myb on the modified electrode was computed from the formula: $Q = nF\Gamma^*$ [25]. The date of Γ^* was $3.0 \times 10^{-9} \text{ mol/cm}^2$, higher than theoretical value ($1.89 \times 10^{-11} \text{ mol/cm}^2$) [26]. Also the total Myb modified on electrode was $4.29 \times 10^{-8} \text{ mol/cm}^2$, so 6.99% of Myb involved in voltammetric reaction. The result revealed that the chain-like AuNCs supplied a conductive interface with long electron transfer path, which was profitable for Myb on electrode surface to transfer electrons.

3.5 Effect of pH

The effect of different buffer pH on the electrochemical behavior of Nafion/Myb/AuNCs/CILE was studied (Fig. 5). The E_{pa} and E_{pc} were moved to the negative potential with increase of pH from

2.0 to 7.0, and the largest I_{pc} was got at pH 2.0, which was selected for the further investigation. Furthermore E^0 had a linearity with pH and the slope (-44.0 mV/pH) was lower than the theoretic data (-59.0 mV/pH). The reason might be the influence of the protonation of water concerted to the central iron. Therefore the DET between Myb and electrode is rendered with the formula: $\text{Myb Fe(III)} + \text{H}^+ + \text{e}^- \rightleftharpoons \text{Myb Fe(II)}$ [27].

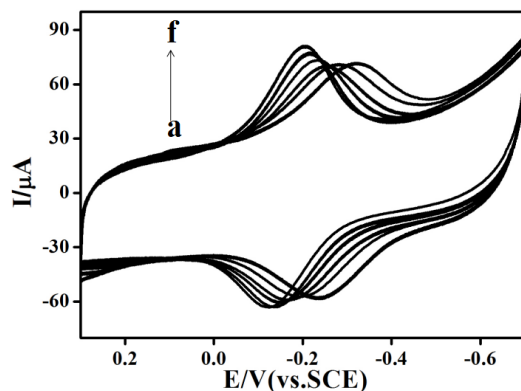


Figure 5. CVs of Nafion/Myb/AuNCs/CILE in 0.1 mol/L PBS at different pH (from a to f: 2.0, 3.0, 4.0, 5.0, 6.0, 7.0) with the scan rate as 100 mV/s.

3.6 Electrocatalytic behavior

Voltammetric responses of Nafion/Myb/AuNCs/CILE to TCA and NaNO_2 were researched. Figure 6A showed CVs of Nafion/Myb/AuNCs/CILE with increasing concentrations of TCA (C_{TCA}). It could be found that a new cathodic peak occurred at -0.503 V (vs. SCE) with C_{TCA} and the decrease of the anodic peak, which was a representative electrochemical reduction process. The linearity of I_{pc} and C_{TCA} was got from 10.0 to 400.0 mmol/L with the regression formula as $I_{pc}(\mu\text{A}) = 5.51 C_{\text{TCA}} (\text{mmol/L}) + 184.8$ ($n=10$, $\gamma=0.992$) and the detection limit as 2.00 mmol/L (3σ). In addition, the apparent Michaelis-Menten constant (K_M^{app}) was got from Lineweaver-Burk equation [28] ($\frac{1}{I_{ss}} = \frac{1}{I_{max}} + \frac{K_M^{\text{app}}}{CI_{max}}$) as 5.7 mmol/L, which was less than the references such as Nafion/Myb-SA-TiO₂/CILE (32.3 mmol/L) [29], CTS-Myb-GR-IL/CILE (8.99 mmol/L) [30], and Nafion/Myb/NiO/GR/CILE (10.67 mmol/L) [31]. The result illustrated that Nafion/Myb/AuNCs/CILE reserved its biological activity and had a well biocompatibility to TCA. A systematic comparison of the electrochemical and analytical parameters of this biosensor with other Myb modified electrodes was listed in table 1, which showed a widely linear range and a relative low detection limit.

Voltammetric catalysis of Nafion/Myb/AuNCs/CILE towards NaNO_2 was investigated with new cathodic peak appeared at -0.588 V with the increase of NaNO_2 (Fig. 6B). A linearity for NaNO_2 concentration versus I_{pc} was achieved as $I_{pc}(\mu\text{A}) = 130.0 C(\text{mmol/L}) + 32.28$ ($n=10$, $\gamma=0.984$) from 0.04 to 1.8 mmol/L. The detection limit was further computed as 0.013 mmol/L (3σ) with K_M^{app} reckoned as 0.76 mmol/L.

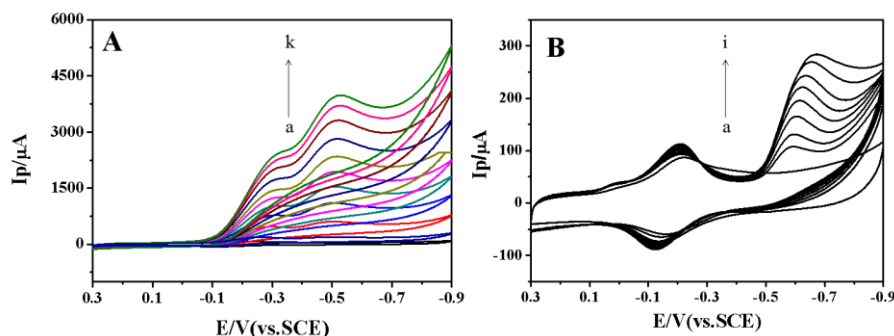


Figure 6. CVs of Nafion/Myb/AuNCs/CILE in the presence of (A) 0, 10, 40, 80, 120, 160, 200, 250, 300, 350, 400 mmol/L TCA (a~k); (B) 0, 0.28, 0.40, 0.60, 0.80, 1.00, 1.20, 1.40, 1.80 mmol/L NaNO_2 (a~i) in pH 2.0 PBS at the scan rate of 100 mV/s.

Table 1. Comparison of electrochemical parameters of different Myb modified electrodes to TCA detection.

Modified electrodes	Linear range (mmol/L)	Detection limit (mmol/L)	K_M^{app} (mmol/L)	Refs.
Nafion/Myb/Cu-BTC/NG/CILE	1.0-460	0.333	13.88	[1]
Nafion/Myb-SA-TiO ₂ /CILE	5.3-114.2	0.152	32.3	[29]
CTS-Myb-GR-IL/CILE	2.0-16.0	0.583	8.99	[30]
Nafion/Myb-SA-Fe ₃ O ₄ -GR/CILE	1.4-119.4	0.174	29.1	[32]
Nafion/Myb/AuNPs/Mg-MOF-74/CILE	1.0-200.0	0.333	9.26	[33]
Nafion/Myb-G-COOH/CILE	5.0-57.0	1.0	1.3	[34]
Nafion/Myb-ACA-GR/CILE	2.5-47.3	0.114	8.3	[35]
Nafion/Myb-SA-GR/CILE	7.5-69.0	0.163	8.71	[36]
Nafion/Myb-Co ₃ O ₄ -Au/IL-CPE	2.0-20.0	0.5	4.7	[37]
Nafion/Myb/AuNCs/CILE	2.0-400.0	0.26	5.7	This Work

3.7 Practical applications

Medical facials peel (35% TCA, Shanghai EKEAR Bio. Tech. Ltd. Co., China) was used as the sample and detected by this method, which were diluted by water and analyzed by the working curve method. The TCA concentration in sample solution was computed and the recoveries were achieved by standard addition method. The analytical data were summarized in table 2 with the recovery from 99.28% to 100.50%, demonstrating the real application of the fabricated working electrode.

Table 2. Analytical results of medical facials peel by the prepared way ($n=3$).

Sample	Detected (mmol/L)	Added (mmol/L)	Total (mmol/L)	Recovery(%)	RSD(%)
35% TCA	207.7	70.00	279.2	100.50	3.5
		100.0	305.5	99.28	0.8
		130.0	337.2	99.86	1.2

4. CONCLUSIONS

In this paper AuNCs was used for the realization of direct electrochemistry of Myb, which was achieved by immobilization of Myb on AuNCs decorated CILE with a Nafion film. Spectroscopic results clarified that Myb reserved its bioactive structure. The utility of high conductive AuNCs with chain-like structure can endow the immobilized Myb to transfer electron with fast rate. A pair of symmetrical redox peaks displayed on the CVs proved the positive effects of AuNCs to electron transfer. The fabricated biosensor revealed well-electrocatalytic activity to reduction of TCA and NaNO_2 . Therefore the method displayed that AuNCs modified electrode could act as a well electrocatalytic biosensing interface for various sensor designs.

ACKNOWLEDGEMENTS

This project was financially supported by the National Natural Science Foundation of Hainan Province of China (2017CXTD007), the Key Science and Technology Program of Haikou City (2017042), National College Students Innovation and Entrepreneurship Training Program (30101100307), and the Open Foundation of Key Laboratory of Water Pollution Treatment and Resource Reuse of Hainan Province (2019-003).

References

1. G. L. Luo, Y. Deng, H. Xie, J. Liu, S. Mi, B. H. Li, G. Li and W. Sun, *Int. J. Electrochem. Sci.*, 14(2019)2732
2. J. Yoon, J. W. Shin, J. Lim, M. Mohammadniaei, G. B. Bapurao, T. Lee and J. W. Choi, *Colloids Surf., B*, 159(2017)729
3. A. Heller, *Acc. Chem. Res.*, 23(1990)128
4. S. M. Chen and C. C. Tseng, *Electrochim. Acta*, 49(2004)1903
5. R. Y. Zou, X. B. Li, G. L. Luo, Y. Y. Niu, W. J. Weng, W. Sun, J. W. Xi, Y. Chen and G. J. Li, *Electroanalysis*, 31(2019)575
6. W. Sun, Y. Q. Guo, T. T. Li, X. M. Ju, J. Lou and C. X. Ruan, *Electrochim. Acta*, , 75(2012)381
7. S. Kang, W. S. Zhao, X. Y. Li, Z. R. Wen, X. L. Niu, B. L. He, L. F. Li and W. Sun, *Int. J. Electrochem. Sci.*, 12(2017)2184
8. K. Saha, S. S. Agasti, C. Kim, X. Li and V. M. Rotello, *Chem. Rev.*, 112(2012)2739
9. A. Murugadoss and A. Chattopadhyay, *J. Phys. Chem. C*, 112(2008)11265
10. W. Xuan, X. Y. He and X. Q. Li, *Sci. Tech. Chem. Ind.*, 26(2018)28.
11. P. Jorge, P. Isabel, L. M. Luis and M. Paul, *Coord. Chem. Rev.*, 249(2005)1870
12. P. Lakshminarayana and Q. H. Xu, *Nanotechnol.*, 19(2008)075601.
13. S. E. Skrabalak, J. Chen, L. Au, X. Lu, X. Li and Y. Xia, *Adv. Mater.*, 19(2010)3177
14. J. Y. Chen, B. J. Wiley and Y. N. Xia, *Langmuir J. Surf. Colloids*, 23(2007)4120
15. N. Nath and A. Chilkoti, *J. Am. Chem. Soc.*, 123(2001)8197
16. A. K. Sinha, M. Basu, S. Sarkar, M. Pradhan and T. Pal, *J. Colloid Interface Sci.*, 398(2013)13
17. X. L. Niu, Z. R. Wen, X. Y. Li, L. J. Yan, W. C. Zhang, S. X. Gong, Z. F. Shi and W. Sun, *Curr. Anal. Chem.*, 13(2017)410
18. D. G. Cameron, J. K. Kauppinen, D. J. Moffatt and H. H. Mantsch, *Appl. Spectrosc.*, 36(1982)245
19. Y. P. Song, M. C. Petty, J. Yarwood, W. J. Feast, J. Tsibouklis and S. Mukherjee, *Langmuir*, 8(1992)257

20. J. F. Rusling and A. E. F. Nassar, *J. Am. Chem. Soc.*, 115(1993)11891
21. W. Sun, D. D. Wang, R. F. Gao and K. Jiao, *Electrochem. Commun.*, 9(2007)1159
22. E. Laviron, *J. Electroanal. Chem.*, 101(1979)19
23. X. Y. Li, X. L. Niu, W. S. Zhao, W. Chen, C. X. Yin, Y. L. Men, G. J. Li and W. Sun, *Electrochem. Commun.*, 86(2017)68
24. X. Q. Li, R. J. Zhao, Y. Wang, X. Y. Sun, W. Sun, C. Z. Zhao and K. Jiao, *Electrochim. Acta*, 55 (2010) 2173
25. D. A. Aikens, *J. Chem. Educ.*, 60(2004)A25
26. S. F. Wang, T. Chen, Z. L. Zhang, D. W. Pang and K. Y. Wong, *Electrochem. Commun.*, 9 (2007) 1709
27. L. Zhang, D. B. Tian and J. J. Zhu, *Bioelectrochemistry*, 74(2008)157
28. R. A. Kamin and G. S. Wilson, *Anal. Chem.*, 52(1980)1198
29. H. Q. Yan, X. Q. Chen, Z. F. Shi, Y. H. Feng, J. C. Li, Q. Lin, X. H. Wang and W. Sun, *J. Solid State Electrochem.*, 20(2016)1783
30. C. X. Ruan, T. T. Li, Q. J. Niu, M. Lu, J. Lou, W. M. Gao and W. Sun, *Electrochim. Acta*, 64 (2012)183
31. W. Sun, S. X. Gong, D. Ying, T. T. Li, Y. Cheng, W. C. Wang and L. Wang, *Thin Solid Films*, 562 (2014)653
32. X. Q. Chen, H. Q. Yan, Z. F. Shi, Y. H. Feng, J. C. Li, Q. Lin, X. H. Wang and W. Sun, *Polym. Bull.*, 74(2016)1
33. G. L. Luo, H. Xie, Y. Y. Niu, J. Liu, Y. Q. Huang, B. H. Li, G. J. Li and W. Sun, *Int. J. Electrochem. Sci.*, 14(2019)2405
34. W. Zheng, W. S. Zhao, W. Chen, W. J. Weng, Z. W. Liao, R. X. Dong, G. J. Li and W. Sun, *Int. J. Electrochem. Sci.*, 12(2017)4341
35. X. Q. Chen, H. Q. Yan, W. Sun, G. Y. Chen, C. J. Yu, W. Feng and Q. Lin, *RSC Adv.*, 8 (2018) 38003
36. X. Q. Chen, M. X. Feng, H. Q. Yan, W. Sun, Z. F. Shi and Q. Lin, *Int. J. Electrochem. Sci.*, 12 (2017) 11633
37. X. F. Wang, Z. You, H. L. Sha, S. X. Gong, Q. J. Niu, and W. Sun, *Microchim. Acta*, 181 (2014)767